Proceedings of Ninth World Conference on Earthquake Engineering
August 2-9, 1988, Tokyo-Kyoto, JAPAN (Vol.IV)

6-2-4

ELASTO-PLASTIC DEFORMATION AND COLLAPSE BEHAVIOR OF BRACING

Bunzo TSUJI

Department of Environmental Planning, Kobe University,
Nada-ku, Rokkodai-cho, Kobe 657 Japan

SUMMARY

To investigate the elasto-plastic deformation and collapse behavior of individual braces with a wide flange cross section, monotonic compressive and alternately repeated cyclic loading tests were performed. Eighteen braces were tested. The effective slenderness ratios of the braces were varied from 30 to 90 and the width-to-thickness ratios from 6 to 13. Influence of flange local buckling on the deterioration of restoring force characteristics of the braces increased as the slenderness ratio decreased. Under cyclic loading, low cycle fatigue cracks appeared at locally buckled flanges or at welded ends of the brace. Deformation capacity of the braces decreased because of these cracks.

INTRODUCTION

To investigate the restoring force characteristics of individual braces subjected to axial forces, many analytical and experimental studies have been performed 1). However, very few data are available on the coupling effect of the local buckling and overall buckling and on the deformation capacity of the braces. Eighteen braces with wide flange cross section and having various slenderness and width-to-thickness ratios of the flanges were tested under monotonically increased compressive and alternately repeated cyclic loadings. Effects of the local buckling of the flange element on the deterioration of strength and deformation capacity of the braces were discussed experimentally. Three braces having a rectangular cross section were also tested with the loading history used in tests for the braces with a wide flange cross section, and the results are compared.

EXPERIMENTAL METHOD

Specimen The specimens tested are shown in Fig.1 and Table 1. Welded built-up wide flange sections and a rectangular cross section were used. At each end of the specimen, a pair of gusset plates were welded to prevent rotation. The effective slenderness ratios of the specimens were from 30 to 90, and the width-to-thickness ratios of the flange elements were from 6.0 to 13.0. Mild steel (SS41) was used, and mechanical properties of the materials tested are shown in Table 2.

Test Setup and Loading Procedure Fig.2 shows the loading system. One end of the specimen is fixed to the rigid block and the other end to the sliding block that can move only in the axial direction. The axial force was applied by an oil

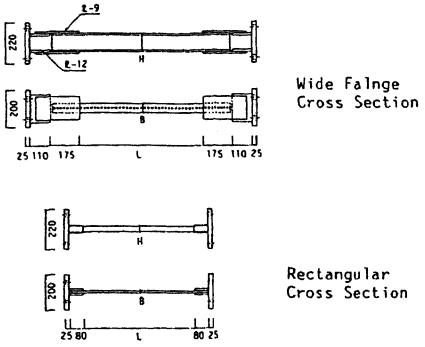

Fig.1 Specimens

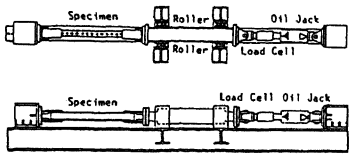

Fig.2 Loading System

Table 1 Specimens Tested

Cross Section	λ	b/t_f	B(mm)	H(mm)	Loading
Wide Flange	30	6	50	100	M, C
		8	50	100	M, C
		10	60	100	M, C
		12	70	100	M, C
		13	80	100	M, C
	60	6	50	100	M, C
		8	50	100	M, C
	90	6	50	100	M, C
		8	50	100	M, C
Rectan-gular	30		12	30	C
	60		12	30	C
	90		12	30	C

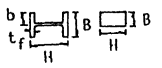

λ : Slenderness Ratio
M : Monotonous Loading
C : Cyclic Loading

Table 2 Mechanical Properties

t(mm)	σ_y(kgf/mm²)	σ_b(kgf/mm²)
3.0	35.5	44.9
3.2	21.0	34.7
4.5	29.9	45.5
12.0	37.0	49.0

t : thickness of plate
σ_y : yield stress
σ_b : tensile strength

jack and measured by a load cell. Monotonic compressive and alternately repeated cyclic axial forces were applied. Fig.3 shows the cyclic loading history. The loading was continued until the specimen was broken.

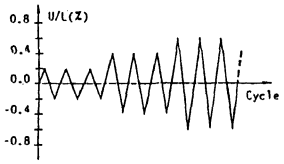

Fig.3 Loading History

EXPERIMENTAL RESULTS

Monotonic Compressive Loading Axial force versus axial displacement relationships obtained for eight braces are shown in Fig.4. The ordinate shows the axial force (N) normarized by the yield axial force (Ny), and the abscissa the axial displacement (U) normarized by the length of brace (L). Symbol,▽, shows the point at which the compression flange was buckled. Axial resistance increases as the slenderness ratio or the width-to-thickness ratio of the flange decreases. As indicated in Fig.4(b), for the braces having a width-to-thickness ratio smaller than 10, overall buckling occured first, and their maximum compressive strengths were approximately 0.95Ny. For the braces having a width-to-thickness ratio not smaller than 10, local buckling preceded the overall buckling. The maximum compressive strengths were approximately 0.80Ny for those braces. The effect of the flange local buckling on the post buckling strength of braces was serious in short braces. Fig.5 shows interactions between the axial force (N) and bending moment (M) for the end and center sections of the brace. The dashed line shows the fully plastic condition of the wide flange section under the axial force and weak axis bending. For the braces having thick flanges, the interaction curves exceeded the fully plastic condition because of the strain hardening effect. For the braces with thin flanges, interaction curves did not exceed the fully plastic condition because of the flange buckling. It was observed, for all braces tested, that both the axial force and bending moment decreased in the large deformation range, because of the local buckling at the flange on the concave side and the cracks at the flange on the convex side.

Alternately Repeated Cyclic Loadings Axial force versus axial displacement

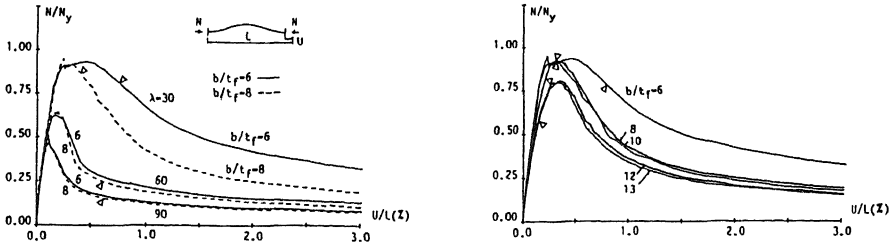

(a) b/t_f=6,8 (b) λ=30

Fig.4 Axial Force vs. Axial Displacement Relationship

relationships obtained for the braces with wide flange cross sections are shown in Fig.6. Symbol, ▼ , shows the points at which a low cycle fatigue crack was first observed. The hysteresis of the brace in tension was of slip type for the braces with the larger slenderness or width-to-thickness ratio. The brace with the slenderness ratio of 30 and width-to-thickness ratio of 12 showed somewhat different behavior. In this brace, only local buckling of the flanges and web was observed, and its strength and stiffness were less deteriorated as compared with the overall buckled braces. Fig.7 shows N-M interaction for cyclic loading tests. For the braces with thick flanges, the curves exceeded the fully plastic condition during the loadings in both tension and compression. The curves of the braces having a width-to-thickness ratio of 10 reached the fully plastic condition only during the loading in tension, but, for the braces with thinner flanges, the curves stayed only inside the fully plastic condition. With the increase in the number of cycles, low cycle fatigue cracks developed, and the curves were made smaller. Fig.8 shows the relationships between the number of cycles and the resistance at the prescribed axial displacement in that cycle. Solid and dashed lines show the compressive and tensile resistances. Except for the first few cycles, the compressive resistance was small for the braces whose slenderness ratio were larger than 60. For the braces with the slenderness ratio of 30, the compressive resistance was kept almost constant until the axial displacement reached 0.5% of its length, and decreased gradually with further increase in the axial displacement. At a given displacement amplitude, the reduction in the tensile resistance after cycles was more significant for slender braces, but the resistance was fully recovered when the axial displacement amplitude was increased. On the other hand, for short braces, the tensile resistance kept decreasing even when the axial displacement amplitude was increased.

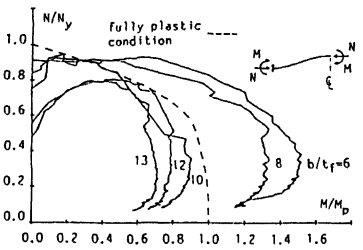

Fig.5 Axial Force vs. Bending Moment Interaction

Braces with Rectangular Cross Section For comparison purposes, cyclic loading tests of braces with a rectangular cross section were also performed. Fig.9 shows the axial force versus axial displacement relationships of the three specimens tested. As the slenderness ratio increased, the hysteresis loops were narrower in width, and slip type behavior was remarkable. Compared with the braces with wide flange cross section, the braces with a rectangular cross section were fractured with a larger displacement. Fig.10 shows the N-M interaction curves. The curves considerably exceeded the fully plastic condition because of the strain hardening effect.

Collapse Behavior The braces subjected to the monotonic loading were collapsed

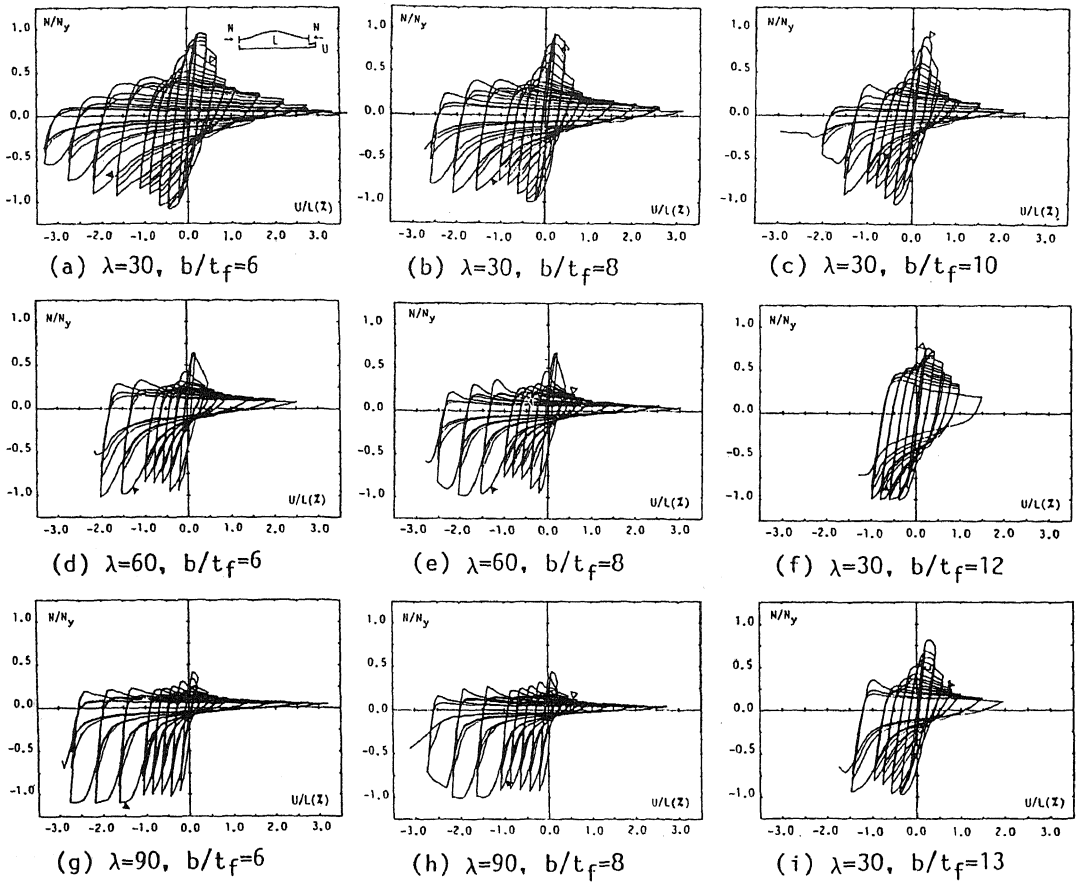

Fig.6 Axial Force vs. Axial Displacement Relationship

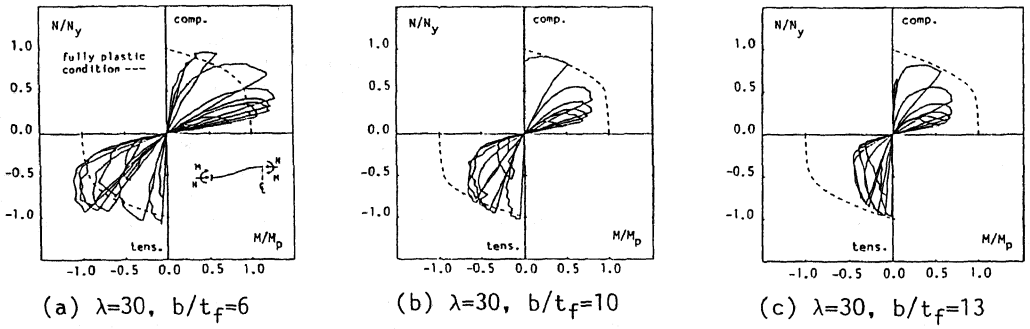

Fig.7 Axial Force vs. Bending Moment Interaction Relationship

in the following manner; first, either local buckling of a flange or overall buckling of the brace occurred; then, the flange on the convex side was cracked. The braces subjected to the cyclic loading were collapsed in following order; first, either overall buckling or local buckling of the flange on the concave side occurred; second, the flange on the convex side was buckled under loading in tension; third, the buckled flange on the concave side was cracked; fourth, the

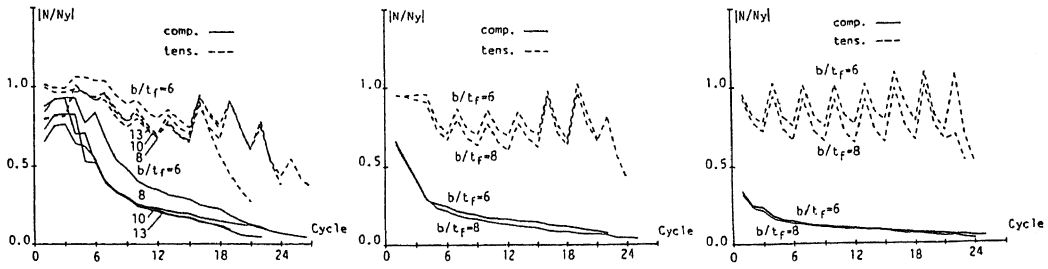

(a) λ=30 (b) λ=60 (c) λ=90

Fig.8 Axial Resistance vs. Loading Cycle Relationship

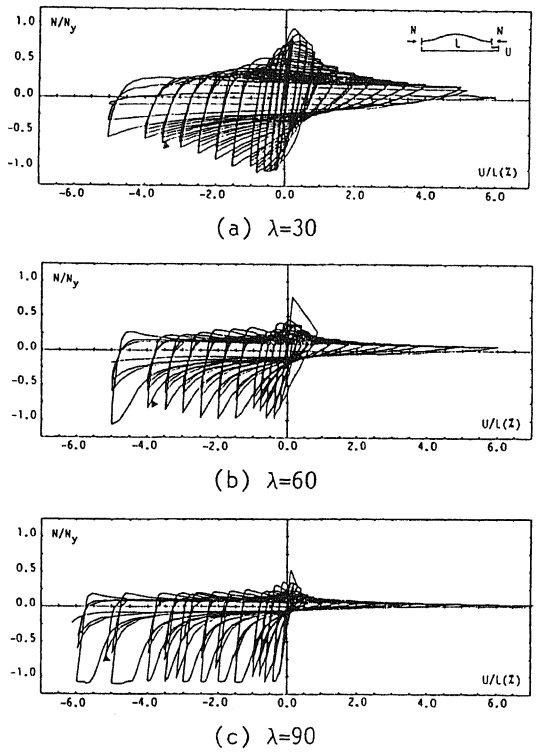

(a) λ=30

(b) λ=60

(c) λ=90

Fig.9 Axial Force vs. Axial Displacement Relationship

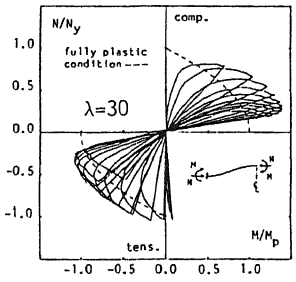

Fig.10 Axial Force vs. Bending Moment Interaction

flange on the convex side was cracked; and finally, the brace was broken. For short members with thin flanges, the flange was buckled at a small axial displacement. The local buckling occurred first at the center of the brace and next at the ends of the brace. Low cycle fatigue cracks were observed first on the concave surface of the locally buckled flange plate and at the flange tip. The cracks on the concave surface progressed rapidly through the thickness of the flange plate, whereas the cracks at the tips progressed gradually through the width of the flange. Except for the brace failed without overall buckling, the collapse mechanism of the braces tested can be classified into the following three types. Type A: the cracks progressed only at both ends of the brace and the brace was broken at one end. Type B: cracks were developed at ends and the center of the brace, and the brace was broken at the center. Type C: cracks were developed only at the center of the brace, and the brace was broken at the center. The long braces with thick flanges collapsed in Type A. Type C was observed in short braces with thin flanges. Other braces were collapsed in Type B. The axial displacement at which the braces were broken were from 2.5 to 3.5 % of their length for Type A and B and from 1.5 to 2.0 % for Type C. For the braces with rectangular cross section, low cycle fatigue cracks were observed first on the concave face, and then on the convex face. These cracks progressed gradually through the depth of the brace, and finally the brace was broken at its center. The displacements at

which the braces were broken were from 6 to 7 % of their length. These displacements were from 2 to 3 times larger than those of the braces with a wide flange cross section.

CONCLUSIONS

Monotonous compressive and alternately repeated cyclic loading tests of the brace with a wide flange cross section and having various slenderness and width-to-thickness ratios of the flanges were performed. Cyclic loading tests of the brace with a rectangular cross section were also conducted. The results obtained from these tests are as follows:

1. The overall buckling force in monotonic loading tests decreased as the effective slenderness ratio of the brace increased.
2. The displacement at which local buckling of the flange occurred decreased as the slenderness ratio decreased or the width-to-thickness ratio of the flange increased. For the braces with the slenderness ratio of 30 and the width-to-thickness ratio greater than 10, local buckling preceded overall buckling.
3. Post buckling strength increased as the slenderness ratio and the width-to-thickness ratio decreased. The effect of the local buckling on the deterioration of the strength was larger for shorter members.
4. Hysteresis loops under the cyclic loading were narrower in width, showing the slip type behavior, as the slenderness and width-to-thickness ratios increased.
5. Under the cyclic loading, the compressive strength was larger as the slenderness and width-to-thickness ratios decreased, and the tensile strength was larger as the width-to-thickness ratio decreased.
6. The interaction curves between the axial force and bending moment exceeded the fully plastic condition because of the strain hardening effect, when the braces had thick flange, whereas the curves stayed only inside the fully plastic condition because of the local buckling effect for the braces in the thin flanges.
7. Three types of the collapse mechanism were observed:
   - Type A: For long braces with thick flanges, low cycle fatigue cracks were developed at both ends of the brace, and the brace was broken at one end.
   - Type B: For relatively short braces with thick flanges, low cycle fatigue cracks were developed at both ends and the center of the brace, and the brace was broken at the center.
   - Type C: For short braces with thin flanges, low cycle fatigue cracks were developed only at the center of the braces, and the brace was broken at the center.
8. The axial displacements at which the braces were broken were from 2.5 to 3.5 % of their length for Type A and B, and from 1.5 to 2.0 % for Type C.
9. The braces with a rectangular cross section were broken at the axial displacement of 6 to 7 % of their length. Those braces had significantly larger deformation capacities as compared with the braces with a wide flange cross section.

REFERENCES

1. Wakabayashi,M.,"Behavior of Braces and Braced Frames," Int. Jour. of Structures, Vol.2, No.2, 49-70, (1982).
2. Tsuji,B., and Nishino,T.,"Elastic Plastic Deformation and Collapse Behavior of Wide flange Bracing," Proc. 7th Japan Earthquake Eng. Symposium, 1381-1386, (1986).